

CERN-TH/2001-161
DESY 01-05

Predictions for $\bar{\nu}\nu\gamma$ Production at LEP

D. Bardin^a, S. Jadach^{b,c,d}, T. Riemann^b and Z. Was^c

^a *Lab. of Nuclear Problems, JINR, RU-141980 Dubna, Russia*

^b *Deutsches Elektronen-Synchrotron DESY, D-15738 Zeuthen, Germany*

^c *Institute of Nuclear Physics, ul. Kawiory 26a, 30-055 Cracow, Poland*

^d *CERN, Theory Division, CH-1211 Geneva 23, Switzerland*

Abstract

We study predictions for the reaction $e^+e^- \rightarrow \bar{\nu}\nu(n\gamma)$. The complete one-loop corrections are taken into account and higher order contributions, in particular those for the observed real photons, are added whenever necessary. The event generator *KKMC*, a general-purpose Monte Carlo generator for the process $e^+e^- \rightarrow \bar{f}f n\gamma$ based on the method of exclusive exponentiation, is used as the environment. We extend its applicability to the process $e^+e^- \rightarrow \bar{\nu}_l \nu_l n\gamma$, $l = e, \mu, \tau$, where the observation of at least a single γ is required. The exponentiation is implemented in much the same way as for the *s*-channel process alone. In particular, all photonic effects present in the case of *W* exchange, which *cannot* be included in the *s*-channel exponentiation scheme, are calculated to a finite order only. The real hard photon matrix element is calculated up to $\mathcal{O}(\alpha^2)$. Leading logarithmic contributions of the two-loop corrections and one-loop photonic corrections accompanying real single photon emission are included. The electroweak corrections are calculated with the *DIZET* library of the *ZFITTER* package. Numerical tests and predictions for typical observables are presented.

Submitted to European Journal of Physics

CERN-TH/2001-161

DESY 01-05

October 2001

Work supported in part by the European Union 5-th Framework under contract HPRN-CT-2000-00149, NATO grant PST.CLG.977751 and INTAS M^o 00-00313.

E-mails: bardin@nusun.jinr.ru, Stanislaw.Jadach@cern.ch, Tord.Riemann@desy.de, Zbigniew.Was@cern.ch

1 Introduction

For the final LEP2 data analysis the total cross-section for the process $e^+e^- \rightarrow \bar{\nu}\nu n\gamma$ will have to be calculated with a precision of 0.5%–1%, and arbitrary differential distributions of observable photons also have to be calculated with similar precision [1]. In future, for a high luminosity linear electron collider like TESLA, the precision requirements will be even more demanding. These requirements may be fulfilled by transferring our expertise from the case of charged lepton production to that of neutrino production, in particular the more involved case of $\bar{\nu}_e \nu_e$ with t -channel exchanges. The present paper marks an important step in this direction. It contains the necessary extensions of the Monte Carlo program \mathcal{KKMC} of ref. [2], originally written for $e^+e^- \rightarrow \bar{f}f$, $f = \mu, \tau, u, d, c, s, b$, to the neutrino case.

In the neutrino pair production process

$$e^+e^- \rightarrow \bar{\nu}\nu n\gamma, \quad (1.1)$$

one is interested in observables where at least one high- p_T photon is observed; neutrinos obviously escape detection. From a methodological point of view, however, it is convenient to consider

$$e^+e^- \rightarrow \bar{\nu}\nu \quad (1.2)$$

as a (non-observable) Born process, and to incorporate (observable) radiative corrections into it, in particular the real photon emissions, which provide the detectable signature. A convenient method of exponentiation is discussed in this framework. In order to achieve the 0.5% precision level for the $\bar{\nu}\nu\gamma$ final state, the leading-logarithmic (LL) corrections have to be calculated up to two or three loops for the virtual corrections and up to two or even three hard photons for multiple bremsstrahlung. Mixed real–virtual terms such as the loop corrections to real photon emission have to be calculated as well¹. Needless to say that a sufficiently precise integration over the multiphoton phase space within the detector acceptance is also necessary. The Monte Carlo (MC) event generator approach is the only practicable solution.

As in the case of any other two-fermion final state in e^+e^- scattering, it is possible to define certain computational building blocks. Our case does not require the complete two-loop effects and we can separate the calculation into two parts: (i) QED: interaction of photons with fermions as well as $WW\gamma$ and $WW\gamma\gamma$ interactions; and (ii) the rest: non-photonic weak and QCD corrections. The type (ii) corrections can be hidden in a few effective coupling constants.

The Monte Carlo method is used for the numerical integration over the Lorentz-invariant phase space, as usual. The Monte Carlo event generator \mathcal{KKMC} is documented in ref. [2]. For a detailed description of its matrix elements for the $e^+e^- \rightarrow \bar{f}f(n\gamma)$ processes we refer the reader to refs. [3, 4].

In section 2 we discuss the implementation of the electroweak corrections. The package **ZFITTER** [5, 6] is used for this purpose. Basic numerical tests of the code in the absence of photonic effects are described.

¹The genuine weak one-loop corrections are sufficient.

In section 3 we introduce the photonic matrix elements. We start from the simplest cases of ν_μ and ν_τ production. We then explain the extension of the matrix elements used in the CEEX exponentiation of refs. [2–4], to the case of $e^+e^- \rightarrow \bar{\nu}_e \nu_e \gamma$. The modifications are due to the presence of t -channel W exchange. We start with the general description of our approximation, and later present the single-photon tree-level amplitude. In particular, we explain how single bremsstrahlung amplitudes are used as a building block in the multiple-photon amplitudes. Finally we briefly explain the calculation (or construction) of our amplitudes for the different higher order cases: one-virtual and one-real photon, and two-real photons.

In section 4, predictions of \mathcal{KK} and KORALZ [7,8] are given for selected observables of the recent LEP MC workshop [1], including results that are used for the final estimate of the theoretical and technical errors of our new calculation.

Section 5 concludes the paper with a statement on the precision of our theoretical predictions for the $\bar{\nu}\nu\gamma$ process, as compared with the precision targets requested by LEP experiments [1].

2 The effective Born approximation for $e^+e^- \rightarrow \bar{\nu}\nu$

Similarly to the case of pure s -channel two-fermion processes, the electroweak one-loop corrections can be incorporated via effective coupling constants of the Z and W to fermions. Let us define here the complete electroweak one-loop corrected effective Born cross-section for neutrino pair production². This is by construction a gauge-invariant quantity. It includes s -channel Z exchange for all three neutrino species, while for ν_e pair production it also includes t -channel W exchange:

$$\frac{d\sigma}{d \cos \vartheta} = \sum_{i=e,\mu,\tau} \frac{d\sigma(e^+e^- \rightarrow \bar{\nu}_i \nu_i)}{d \cos \vartheta} = 3 \sigma_s + \sigma_{st} + \sigma_t. \quad (2.1)$$

The improved Born cross-section originates from a neutral-current matrix element \mathcal{M}_Z [5,9],

$$\mathcal{M}_Z = \frac{G_\mu}{2\sqrt{2}} \rho_{e\nu}^Z \chi_Z(s) [\bar{u}_e \gamma_\mu (\bar{v}_e + \gamma_5) u_e] \times [\bar{u}_\nu \gamma_\mu (1 + \gamma_5) u_\nu], \quad (2.2)$$

and, for $\bar{\nu}_e \nu_e$ production only, additionally from a charged-current matrix element \mathcal{M}_W [10]:

$$\mathcal{M}_W = \frac{G_\mu}{\sqrt{2}} \rho_{e\nu_e}^W \chi_W(t) [\bar{u}_e \gamma_\mu (1 + \gamma_5) u_e] \times [\bar{u}_\nu \gamma_\mu (1 + \gamma_5) u_\nu]. \quad (2.3)$$

We use here the notations $a_e = a_\nu = 1$, $Q_e = -1$, $s_W^2 = 1 - M_W^2/M_Z^2$, and have only three form factors κ_e , $\rho_{e\nu}^Z$, and $\rho_{e\nu_e}^W$:

$$\bar{v}_e = 1 - 4|Q_e|s_W^2 \kappa_e. \quad (2.4)$$

²The notations in this section follow closely those of the package ZFITTER.

In the Born approximation, it is $\rho = \kappa = 1$. The kinematical invariants are used in the approximation $m_e = 0$:

$$t = -\frac{s}{2}(1 - \cos \vartheta), \quad (2.5)$$

$$u = -s - t = -\frac{s}{2}(1 + \cos \vartheta). \quad (2.6)$$

We also use:

$$\chi_B(s) = \frac{M_B^2}{-s + M_B^2(s)}, \quad (2.7)$$

$$M_B^2(s) = M_B^2 - iM_B \Gamma_B(s) \theta(s), \quad (2.8)$$

and the width in the s -channel may be chosen constant or s -dependent. The resulting cross-section contributions are:

$$\sigma_s = \frac{sG_\mu^2}{128\pi} |\chi_Z(s) \rho_{e\nu}^Z|^2 \left[(1 + \cos^2 \vartheta) (1 + |v_e|^2) + 4 \cos \vartheta \operatorname{Re} v_e \right], \quad (2.9)$$

$$\sigma_{st} = -\frac{sG_\mu^2}{32\pi} \operatorname{Re} \left\{ \chi_Z(s) \chi_W^*(t) \rho_{e\nu}^Z \rho_{e\nu}^{W*} (1 + \cos \vartheta)^2 (1 + v_e) \right\}, \quad (2.10)$$

$$\sigma_t = \frac{sG_\mu^2}{16\pi} |\chi_W(t) \rho_{e\nu}^W|^2 (1 + \cos \vartheta)^2. \quad (2.11)$$

The weak neutral form factors κ_e and $\rho_{e\nu}^Z$ are discussed in detail in [5, 11] and in references therein³. For latest comparisons and applications at LEP1, see also [12], and at LEP2, see ref. [1]. There is one modification with respect to earlier applications, which has to be clarified here. Even though the complete virtual corrections are not infrared-finite (because of photonic diagrams), we prefer *not* to split away the photonic part of the virtual corrections in our formulae. Instead, we prefer to combine the complete virtual corrections with real bremsstrahlung from the package⁴ \mathcal{KK} MC. For this reason, we calculate with the weak library `DIZET` of the package `ZFITTER` the complete virtual correction $\rho_{e\nu}^Z$. Since in the quantity `XROK(1)` the QED part is explicitly subtracted, we have to re-establish its contribution here according to the formula:

$$\rho_{e\nu}^Z = \text{XROK}(1) + \text{QED_NC}, \quad (2.12)$$

$$\text{QED_NC} = \frac{\alpha}{2\pi} Q_e^2 \left[-(L_e - 1) \ln \frac{m_e^2}{\lambda^2} - \frac{1}{2} L_e^2 + \frac{3}{2} L_e + 4 \operatorname{Li}_2(1) - 2 \right], \quad (2.13)$$

with $L_e = \ln(s/m_e^2)$ and λ a finite photon mass.

The charged current form factor may be extracted from derivations done for ep scattering [13–15]. Again, an infrared-finite quantity `ROWB`⁵ was constructed, rather than the full

³These form factors are calculated in the library `DIZET` as variables `XROK(2)` and `XROK(1)` by calling subroutine `ROKANC(u, -s, t)` for $s > 0$ and $t, u < 0$.

⁴Of course \mathcal{KK} MC includes virtual QED corrections of its own. The subtraction of the QED part from the complete loop corrections will be defined in section 2.1.

⁵With a call on subroutine `RHOCC(u, -t, s)` (for $s > 0$ and $t, u < 0$). This infrared-finite term was determined by a subtraction of (gauge-dependent) photonic corrections, which were combined for applications at HERA with real-photon corrections. Note also that we use for this part the names of subroutines (but not of variables) from the package `HECTOR` [10].

form factor $\rho_{e\nu}^W$:

$$\rho_{e\nu}^W = \text{ROWB} + \text{QED_CC}, \quad (2.14)$$

$$\text{QED_CC} = \frac{\alpha}{2\pi} Q_e^2 \left[-(L_e - 1) \ln \frac{m_e^2}{\lambda^2} - \frac{1}{2} L_e^2 + \frac{3}{2} \ln \frac{M_W^2}{m_e^2} + \frac{1}{2} \ln^2 \frac{t}{s} \right]. \quad (2.15)$$

For practical reasons, we have decided to insert the neutral current term QED_NC (instead of QED_CC) also in the charged current case:

$$\rho_{e\nu}^W = \text{ROWB}' + \text{QED_NC}, \quad (2.16)$$

$$\text{ROWB}' = \text{ROWB} + \text{QED_CC} - \text{QED_NC}. \quad (2.17)$$

All the virtual corrections described here come with **ZFITTER** v.6.36 (21 June 2001) [5, 6].

2.1 Form factors and \mathcal{KK}

The effects due to the loop diagrams given in formulae (2.12) and (2.16) are separated into the finite parts, which are encapsulated in two of the electroweak form factors and pretabulated in \mathcal{KK} in order to save computer time, and the infrared-divergent part QED_NC which defines the (now universal) genuine QED corrections. The term QED_NC is not included in the form factors, but enter the QED part of the calculation (encapsulated in \mathcal{KK} MC). The remaining finite parts modify Z and W couplings to fermions as in Refs. [3, 4].

We are currently not aiming yet at a calculation of the complete second-order corrections. We may, therefore, incorporate the difference between the QED parts for s - and t -channel

$$\delta_{\text{CC-NC}} = \text{QED_CC} - \text{QED_NC} = \frac{\alpha}{2\pi} Q_e^2 \left[\frac{3}{2} \ln \frac{M_W^2}{s} + \frac{1}{2} \ln^2 \frac{t}{s} - 4 \text{Li}_2(1) + 2 \right] \quad (2.18)$$

into the electroweak formfactor ROWB' , as mentioned above. The difference (2.18) is infrared-finite, numerically small, and not enhanced by the large logarithms with respect to $\frac{\alpha}{2\pi}$. The numerical contribution is in fact below 0.5% of the Born cross section for LEP2 energies, when integrated over neutrino angular variables.

2.2 Technical tests for the “academic” event selection

Before the actual discussion of the bremsstrahlung part of the generator, let us make certain elementary numerical tests of the implementation of the $\rho_{e\nu}^W$ function of eq. (2.16) within the \mathcal{KK} MC program. This will include the neutral current form factors as well, and will be done with the aid of the semi-analytical package \mathcal{KK} sem, the internal testing program of \mathcal{KK} MC. As a first step we compare the effective Born predictions as calculated by \mathcal{KK} sem and by **ZFITTER**. In table 1 we present the predictions from the two programs for the processes $e^+e^- \rightarrow \mu^+\mu^-$, $e^+e^- \rightarrow \bar{\nu}_\mu \nu_\mu$, and finally for the processes $e^+e^- \rightarrow \bar{\nu}_e \nu_e$. In all cases the agreement between \mathcal{KK} sem and **ZFITTER** we find to be sufficiently good, slightly less precise in case of $e^+e^- \rightarrow \bar{\nu}_e \nu_e$. In the latter case possible uncertainties of numerical integration (and pretabulation) can be the reason, as the distributions of the scattering angle peaks in the forward region. We conclude that the program \mathcal{KK} MC properly exploits the electroweak form factors of the package **DIZET**. This opens the way to a more complete treatment of the EW corrections in \mathcal{KK} MC for the neutrino channels.

Table 1: Electroweak effects including pretabulation as implemented in \mathcal{KK} MC. Total cross-sections and forward-backward asymmetries are calculated without QED corrections. For every total energy the upper entry is from \mathcal{KK} sem and the lower one from ZFITTER .

Channel	Cms energy [GeV]	σ	A_{FB}
$e^+e^- \rightarrow \mu^+\mu^-$	91.19	2.00345818887006	0.01782302636524
		2.00339325242333	0.01783385260585
	100.00	0.05261755867120	0.58632495479977
		0.05261818913548	0.58632716129114
	140.00	0.00697974693325	0.66477236253951
		0.00697977362831	0.66477185420337
	189.00	0.00337662390496	0.56552465469245
		0.00337666453508	0.56552686535458
	200.00	0.00298389425320	0.55492797790038
		0.00298394853103	0.55493448086923
	206.00	0.00279941156110	0.54984466446977
		0.00279947462003	0.54985275218873
$e^+e^- \rightarrow \bar{\nu}_\mu \nu_\mu$	91.19	3.97432928812849	0.10951545488039
		3.97416166784039	0.10954931699922
	100.00	0.08476335609986	0.10779125894503
		0.08476366520697	0.10782386820347
	140.00	0.00375688589078	0.10221239752831
		0.00375689763895	0.10224383875601
	189.00	0.00115026771057	0.09199984287991
		0.00115029626002	0.09203384569328
	200.00	0.00096201292991	0.08639737806323
		0.00096202811147	0.08642343541349
	206.00	0.00087902320002	0.08379052580837
		0.00087903346591	0.08381353397919
$e^+e^- \rightarrow \bar{\nu}_e \nu_e$	91.19	3.98484724572530	0.11158999944974
		3.98468359582307	0.11162475358080
	100.00	0.15558776383424	0.44218368752900
		0.15560448223749	0.44225943946968
	140.00	0.04084986326864	0.82963857483597
		0.04086399163970	0.82969877450851
	189.00	0.03937265031133	0.91661747898646
		0.03939257132943	0.91665886557827
	200.00	0.03971937632138	0.92595698881602
		0.03974060496062	0.92599592232744
	206.00	0.03993258937665	0.93040498709775
		0.03995453232877	0.93044271454420

3 Exponentiation and t -channel W -exchange

The coherent exclusive exponentiation (CEEX) was introduced in refs. [3, 4]. It is deeply rooted in the Yennie Frautschi Suura (YFS) exponentiation [16], and for applications to narrow resonances see also earlier related refs. [17, 18]. The exponentiation procedure, i.e.

the re-organization of the QED perturbative series such that infrared (IR) divergences are summed up to infinite order, is done for both real and virtual emissions at the spin-amplitude level (the case of CEEX), while the actual cancellation of the IR divergences always occurs at the integrated cross-section level. CEEX is an extension of the traditional YFS exponentiation, in the sense that, in the standard YFS exponentiation (which we call EEX – for exclusive exponentiation), the isolation of the real IR divergences is done after squaring and spin-summing spin amplitudes, while in CEEX it is done before. In the actual implementation of the CEEX, all spin amplitudes for the fermion pair production in electron–positron scattering are handled with help of the powerful Weyl spinor (WS) techniques. There are several variants of the WS techniques. We have chosen the method of Kleiss and Stirling (KS) [19, 20], because we found KS method well suited for constructing the multiphoton spin amplitudes. In refs. [3, 4] more details of the approach are available. In particular we take all notations and definitions from these works. In the following we recall only the very basic formulae of refs. [3, 4], before we show how the multiphoton CEEX spin amplitudes for the W contribution t -channel is constructed and calculated.

3.1 The master formula

Defining the Lorentz-invariant phase space as

$$\int d\text{Lips}_n(P; p_1, p_2, \dots, p_n) = \int (2\pi)^4 \delta(P - \sum_{i=1}^n p_i) \prod_{i=1}^n \frac{d^3 p_i}{(2\pi)^3 2p_i^0}, \quad (3.1)$$

we write the general CEEX total cross-section for the process

$$e^+(p_a) + e^-(p_b) \rightarrow f(p_c) + \bar{f}(p_d) + \gamma(k_1) + \gamma(k_2) + \dots + \gamma(k_n), \quad n = 0, 1, 2, \dots, \infty, \quad (3.2)$$

with polarized beams and decays of unstable final fermions being sensitive to fermion spin polarizations (neutrinos are, of course, taken as stable), as follows [3]:

$$\sigma^{(r)} = \frac{1}{\text{flux}(s)} \sum_{n=0}^{\infty} \int d\text{Lips}_{n+2}(p_a + p_b; p_c, p_d, k_1, \dots, k_n) \rho_{\text{CEEX}}^{(r)}(p_a, p_b, p_c, p_d, k_1, \dots, k_n) \quad (3.3)$$

where

$$\begin{aligned} \rho_{\text{CEEX}}^{(r)}(p_a, p_b, p_c, p_d, k_1, k_2, \dots, k_n) &= \frac{1}{n!} e^{Y(\Omega; p_a, \dots, p_d)} \bar{\Theta}(\Omega) \sum_{\sigma_i=\pm 1} \sum_{\lambda_i, \bar{\lambda}_i=\pm 1} \\ &\sum_{i,j,l,m=0}^3 \hat{\varepsilon}_a^i \hat{\varepsilon}_b^j \sigma_{\lambda_a \bar{\lambda}_a}^i \sigma_{\lambda_b \bar{\lambda}_b}^j \mathfrak{M}_n^{(r)} \left(\begin{smallmatrix} p_1 k_1 & p_2 k_2 & \dots & p_n k_n \\ \lambda \sigma_1 \sigma_2 & \lambda \sigma_2 \sigma_3 & \dots & \lambda \sigma_n \end{smallmatrix} \right) [\mathfrak{M}_n^{(r)} \left(\begin{smallmatrix} p_1 k_1 & p_2 k_2 & \dots & p_n k_n \\ \bar{\lambda} \sigma_1 \sigma_2 & \bar{\lambda} \sigma_2 \sigma_3 & \dots & \bar{\lambda} \sigma_n \end{smallmatrix} \right)]^* \sigma_{\bar{\lambda}_c \lambda_c}^l \sigma_{\bar{\lambda}_d \lambda_d}^m \hat{h}_c^l \hat{h}_d^m. \end{aligned} \quad (3.4)$$

Assuming the dominance of the s -channel exchanges, including resonances, we define the complete set of spin amplitudes for the emission of n photons in $\mathcal{O}(\alpha^r)_{\text{CEEX}}$ ($r = 0, 1, 2$) as

follows:

$$\begin{aligned}
\mathfrak{M}_n^{(0)} \left(\begin{smallmatrix} p & k_1 \\ \lambda & \sigma_1 \end{smallmatrix} \dots \begin{smallmatrix} p & k_n \\ \lambda & \sigma_n \end{smallmatrix} \right) &= \sum_{\wp \in \{I, F\}^n} \prod_{i=1}^n \mathfrak{s}_{[i]}^{\{\wp_i\}} \beta_0^{(0)} \left(\begin{smallmatrix} p \\ \lambda \end{smallmatrix}; X_\wp \right), \\
\mathfrak{M}_n^{(1)} \left(\begin{smallmatrix} p & k_1 \\ \lambda & \sigma_1 \end{smallmatrix} \dots \begin{smallmatrix} p & k_n \\ \lambda & \sigma_n \end{smallmatrix} \right) &= \sum_{\wp \in \{I, F\}^n} \prod_{i=1}^n \mathfrak{s}_{[i]}^{\{\wp_i\}} \left\{ \beta_0^{(1)} \left(\begin{smallmatrix} p \\ \lambda \end{smallmatrix}; X_\wp \right) + \sum_{j=1}^n \frac{\beta_1^{(1)} \left(\begin{smallmatrix} p & k_j \\ \lambda & \sigma_j \end{smallmatrix}; X_\wp \right)}{\mathfrak{s}_{[j]}^{\{\wp_j\}}} \right\}, \\
\mathfrak{M}_n^{(2)} \left(\begin{smallmatrix} p & k_1 \\ \lambda & \sigma_1 \end{smallmatrix} \dots \begin{smallmatrix} p & k_n \\ \lambda & \sigma_n \end{smallmatrix} \right) &= \sum_{\wp \in \{I, F\}^n} \prod_{i=1}^n \mathfrak{s}_{[i]}^{\{\wp_i\}} \left\{ \beta_0^{(2)} \left(\begin{smallmatrix} p \\ \lambda \end{smallmatrix}; X_\wp \right) + \sum_{j=1}^n \frac{\beta_1^{(2)} \left(\begin{smallmatrix} p & k_j \\ \lambda & \sigma_j \end{smallmatrix}; X_\wp \right)}{\mathfrak{s}_{[j]}^{\{\wp_j\}}} + \sum_{1 \leq j < l \leq n} \frac{\beta_2^{(2)} \left(\begin{smallmatrix} p & k_j & k_l \\ \lambda & \sigma_j & \sigma_l \end{smallmatrix}; X_\wp \right)}{\mathfrak{s}_{[j]}^{\{\wp_j\}} \mathfrak{s}_{[l]}^{\{\wp_l\}}} \right\}.
\end{aligned} \tag{3.5}$$

In the following, we will explain only those aspects of the above formulae that are new for the t -channel W -boson implementations (e.g. the phase space and general form of terms will remain untouched); for all the rest we refer the reader to refs. [3, 4]. We will start from the simplest case and consecutively explain how to add more complicated terms.

Obviously, since only initial-state bremsstrahlung contributes, sums over the partitions drops out. The emissions from W bosons (if present) will not be treated as an additional source of emission requiring a special partition for itself. It will play the role of a correction to the (infrared-finite) β -functions at any perturbative order.

3.2 Case of ν_μ and ν_τ production

For all neutrino flavours except ν_e , we can limit ourselves to changes of the numerical values of the Z couplings from quarks or leptons to neutrinos. All the formulae remain unchanged otherwise, and the previously estimated precisions for the muon channel remain valid also for the neutrino case. The only new element is that of the implementation of electroweak form factors for the neutrinos. They were not investigated for the neutrino channel until the present paper, for DIZET being either a weak library of \mathcal{KK} MC or a stand-alone code.

3.3 The ν_e implementation, general aims

In the case of calculations performed at any fixed order, there is, in principle, no need to worry about gauge invariance, cancellation of infrared or ultraviolet singularities, etc. However, in practice it is sometimes quite non-trivial to achieve these essentials. Already the introduction of the W and Z boson propagators require summation of infinite series of partial contributions from any order of the perturbation expansion. Otherwise, the cross-sections at the peak of e.g. the Z resonance would not be well defined. There are standard techniques, such as the renormalization group, structure functions, and exponentiation, for summing up leading higher-order terms arising from ultraviolet, infrared, or collinear singularities.

Our ambitions here are rather limited. We want to exploit the relative similarity of the spin amplitudes involving t -channel W exchange and s -channel Z exchange at relatively low

energies. Even though diagrams for electron neutrino pair production involving W exchange with photon lines attached only to electron lines are not gauge-invariant (contrasting with the case with the analogous s -channel Z exchange), the necessary contribution for completing the gauge-invariant amplitude is small (and even vanishes within the LL approximation). W -exchange also drops out at sufficiently low energies, where it is legitimately approximated as a contact interaction. As a first step, we shall exploit the simplified amplitudes for the W -exchange in the contact interaction approximation, which formally will look exactly the same as the contribution of an additional heavy Z' . As a second step we shall calculate the difference of the correct/complete perturbative results at fixed, first and second order, with the above approximation. In such a two-step procedure we can easily use the already developed and tested formulation for the s -channel CEEX and the corresponding program code. In addition, we shall also be capable dividing the W -exchange amplitude into individually gauge-invariant parts of a well-defined physical origin.

In the following we will explain our approach in more detail. We start with a common technical trick exploiting Fierz transformation: for massless neutrinos it is possible to rearrange the lowest order $e^+e^- \rightarrow \nu\bar{\nu}$ W -exchange amplitude into a form identical to the one for Z' production exchange, except that the propagator now depends on t and the coupling constants are redefined. The complete Born-level spin amplitude then reads

$$\begin{aligned}
\mathfrak{B}^p_{(\lambda)}(X) &= \mathfrak{B}^p_{(\lambda_a \lambda_b \lambda_c \lambda_d)}(X) = \mathfrak{B}^p_{[\lambda_b \lambda_a]} \mathfrak{B}^p_{[\lambda_c \lambda_d]}(X) = \mathfrak{B}_{[bc][cd]}(X) = \\
&= ie^2 \sum_{B=\gamma, Z, W} \Pi_B^{\mu\nu}(X) (G_{e,\mu}^B)_{[ba]} (G_{f,\nu}^B)_{[cd]} H_B = \sum_{B=\gamma, Z, W} \mathfrak{B}_{[bc][cd]}^B(X), \\
(G_{e,\mu}^B)_{[ba]} &\equiv \bar{v}(p_b, \lambda_b) G_{e,\mu}^B u(p_a, \lambda_a), \quad (G_{f,\mu}^B)_{[cd]} \equiv \bar{u}(p_c, \lambda_c) G_{f,\mu}^B v(p_d, \lambda_d), \\
G_{e,\mu}^B &= \gamma_\mu \sum_{\lambda=\pm} \omega_\lambda g_\lambda^{B,e}, \quad G_{f,\mu}^B = \gamma_\mu \sum_{\lambda=\pm} \omega_\lambda g_\lambda^{B,f}, \quad \omega_\lambda = \frac{1}{2}(1 + \lambda \gamma_5), \\
\Pi_{B=\gamma, Z}^{\mu\nu}(X) &= \frac{g^{\mu\nu}}{X^2 - M_B^2 + i\Gamma_B X^2/M_B}, \\
\Pi_{B=W}^{\mu\nu}(X) &= \frac{g^{\mu\nu}}{t_0 - M_W^2}.
\end{aligned} \tag{3.6}$$

Similarly to the case of Z and γ exchanges, described in ref. [4], the W contribution takes the following form:

$$\mathfrak{B}_{[ba][cd]}^W(X) = 2ie^2 \frac{\delta_{\lambda_a, -\lambda_b} \left[g_{\lambda_a}^{W,e} g_{-\lambda_a}^{W,f} T_{\lambda_c \lambda_a} T'_{\lambda_b \lambda_d} + g_{\lambda_a}^{W,e} g_{\lambda_a}^{W,f} U'_{\lambda_c \lambda_b} U_{\lambda_a \lambda_d} \right]}{t - M_W^2}, \tag{3.7}$$

where t is calculated uniquely for every individual event from the 4-momenta of⁶ $e^+, e^-, \nu, \bar{\nu}$, $g_{\lambda=-1,1}^{W,e} = -\frac{1}{\sqrt{2} \sin \theta_W}$, 0 and $g_{\lambda=-1,1}^{W,\nu_e} = 0, \frac{1}{\sqrt{2} \sin \theta_W}$.

Let us now consider the amplitudes involving the emission of real photons. We also apply the Fierz transformation. The contribution \mathfrak{B}^W is then added at *any* place where the standard Z contribution (eq. (44) of ref. [4]) occurs – that is, in the definition of all $\beta_i^{(j)}$. Note that such an approximation can be used at any order of the perturbation expansion. This approximation preserves gauge invariance, because the resulting spin amplitudes look formally as a

⁶Except some contributions to $\beta_1 \beta_2$, where the “correct” transfers involving momenta of the photons has to be re-established. See discussion below.

contribution from an additional heavy Z' , with the appropriately chosen coupling constants and propagators.

The recipe for extending the \mathcal{KK} MC amplitudes to the ν_e -pair production at this introductory level is relatively simple: modify eq. (43) of ref. [4] and use it later on as a building block for all other amplitudes, virtual corrections and hard bremsstrahlung alike⁷. For the processes at low energies (substantially lower than 80 GeV CMS energy) such an approximation coincides with the standard approximation of the contact interaction, where the momentum transfer is completely neglected in the W propagators and the $W-\gamma$ vertices are neglected.

At higher energies, we have to take the t -channel transfer into account; this modifies the structure of the amplitudes significantly. We may still, as an intermediate solution, introduce an auxiliary single “mean” (“effective”) transfer t_0 for the entire amplitude (including propagators in loop diagrams). With such an auxiliary transfer, the structure of the whole set of spin amplitudes still coincides with the one for s -channel processes, provided that we also drop all $W-\gamma$ interactions. The introduction of such an auxiliary transfer t_0 is the source of certain ambiguity in the case of an event with hard photons. The optimal choice of t_0 should, of course, minimize the unaccounted higher-order corrections.

At present, the routine `KinLib_ThetaD` of \mathcal{KK} MC is used to define the transfer t_0 , the same as for the calculation of the θ -dependent box corrections in the earlier published versions of the \mathcal{KK} MC.

3.3.1 One real photon

The starting point is the well-known $\mathcal{O}(\alpha)$ spin amplitude for the single-photon bremsstrahlung. We have to consider it anew, because we need it in conventions of ref. [4]. In particular we need to keep track of the relative complex phases of parts of the amplitude, which enter the soft photon factors and the remaining finite parts. Also, we want to (re)use the part of the amplitude for ν_μ channel in the ν_e case without any modifications. This will be a starting point for obtaining $\hat{\beta}_1^{(0)}$ of eq. (3.5), which will be later incorporated into our general scheme of exponentiation, exactly as explained in [4].

The first-order matrix element from the Feynman diagrams depicted in fig. 1 reads

$$\begin{aligned}
\mathcal{M}_{\{I\}} \left(\begin{smallmatrix} p_{k_1} \\ \lambda \sigma_1 \end{smallmatrix} \right) = & e Q_e \bar{v}(p_b, \lambda_b) \mathbf{M}_{\{I\}}^{ba} \frac{\not{p}_a + m - \not{k}_1}{-2k_1 p_a} \not{\epsilon}_{\sigma_1}^*(k_1) u(p_a, \lambda_a) \\
& + e Q_e \bar{v}(p_b, \lambda_b) \not{\epsilon}_{\sigma_1}^*(k_1) \frac{-\not{p}_b + m + \not{k}_1}{-2k_1 p_b} \mathbf{M}_{\{I\}}^{ac} u(p_a, \lambda_a) \\
& + e \bar{v}(p_b, \lambda_b) \mathbf{M}_{\{I\}}^{bd,ac} u(p_a, \lambda_a) \not{\epsilon}_{\sigma_1}^*(k_1) \cdot (p_c - p_a + p_b - p_d) \\
& + e \bar{v}(p_b, \lambda_b) g_{\lambda_b, \lambda_d}^{We\nu} \not{\epsilon}_{\sigma_1}^*(k_1) v(p_d, \lambda_d) \bar{u}(p_c, \lambda_c) g_{\lambda_c, \lambda_a}^{We\nu} \not{k}_1 u(p_a, \lambda_a) \\
& - e \bar{v}(p_b, \lambda_b) g_{\lambda_b, \lambda_d}^{We\nu} \not{k}_1 v(p_d, \lambda_d) \bar{u}(p_c, \lambda_c) g_{\lambda_c, \lambda_a}^{We\nu} \not{\epsilon}_{\sigma_1}^*(k_1) u(p_a, \lambda_a),
\end{aligned} \tag{3.8}$$

⁷In the program this is realized by calling subroutine `GPS_BornWPplus` from subroutine `GPS_BornPlus`.

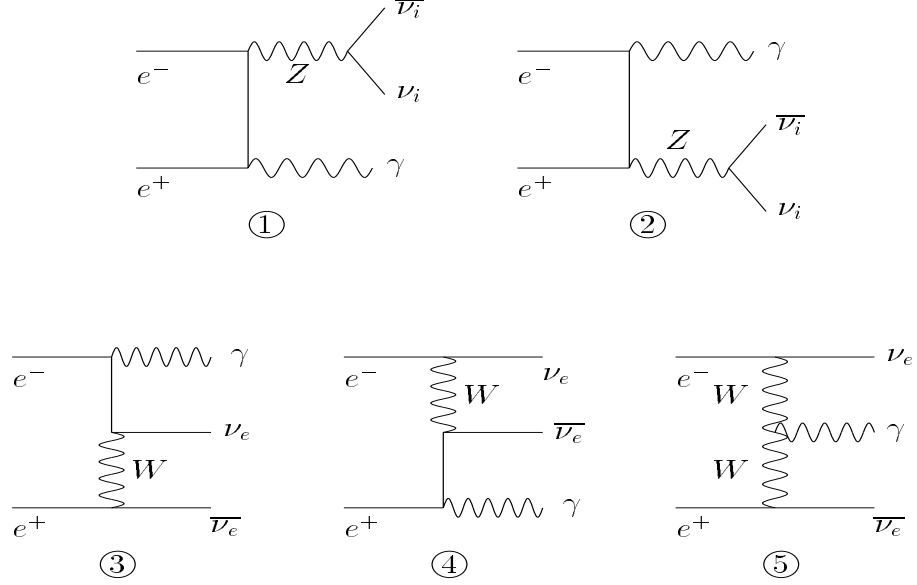


Figure 1: The Feynman diagrams for $e^+e^- \rightarrow \bar{\nu}_e \nu_e \gamma$.

or, equivalently, as follows:

$$\begin{aligned}
\mathcal{M}_{\{I\}} \binom{p_{k_1}}{\lambda_{\sigma_1}} &= \mathcal{M}^0 + \mathcal{M}_{WW\gamma}^1 + \mathcal{M}_{WW\gamma}^2 + \mathcal{M}_{WW\gamma}^3 \\
\mathcal{M}^0 &= e Q_e \bar{v}(p_b, \lambda_b) \mathbf{M}_{\{I\}}^{bd} \frac{\not{p}_a + m - \not{k}_1}{-2k_1 p_a} \not{\epsilon}_{\sigma_1}^*(k_1) u(p_a, \lambda_a) \\
&+ e Q_e \bar{v}(p_b, \lambda_b) \not{\epsilon}_{\sigma_1}^*(k_1) \frac{-\not{p}_b + m + \not{k}_1}{-2k_1 p_b} \mathbf{M}_{\{I\}}^{ac} u(p_a, \lambda_a) \\
\mathcal{M}^1 &= +e \bar{v}(p_b, \lambda_b) \mathbf{M}_{\{I\}}^{bd,ac} u(p_a, \lambda_a) \not{\epsilon}_{\sigma_1}^*(k_1) \cdot (p_c - p_a + p_b - p_d) \frac{1}{t_a - M_W^2} \frac{1}{t_b - M_W^2}, \\
\mathcal{M}^2 &= +e \bar{v}(p_b, \lambda_b) g_{\lambda_b, \lambda_d}^{We\nu} \not{\epsilon}_{\sigma_1}^*(k_1) v(p_d, \lambda_d) \bar{u}(p_c, \lambda_c) g_{\lambda_c, \lambda_a}^{We\nu} \not{k}_1 u(p_a, \lambda_a) \frac{1}{t_a - M_W^2} \frac{1}{t_b - M_W^2} \\
\mathcal{M}^3 &= -e \bar{v}(p_b, \lambda_b) g_{\lambda_b, \lambda_d}^{We\nu} \not{k}_1 v(p_d, \lambda_d) \bar{u}(p_c, \lambda_c) g_{\lambda_c, \lambda_a}^{We\nu} \not{\epsilon}_{\sigma_1}^*(k_1) u(p_a, \lambda_a) \frac{1}{t_a - M_W^2} \frac{1}{t_b - M_W^2}, \tag{3.9}
\end{aligned}$$

where

$$\mathbf{M}_{\{I\}}^{xy} = ie^2 \sum_{B=W,Z} \Pi_B^{\mu\nu}(X) G_{e,\mu}^B (G_{f,\nu}^B)_{[cd]} \tag{3.10}$$

is the annihilation scattering spinor matrix, including final-state spinors and

$$g_{\lambda_c, \lambda_a}^{We\nu} = e \frac{1}{\sqrt{2} \sin \theta_W} \delta_{\lambda_a}^{\lambda_c} \delta_{+}^{\lambda_c}. \tag{3.11}$$

For the W contribution, the subscripts in $\mathbf{M}_{\{I\}}$ define the momentum transfer in the W propagator $\Pi_W^{\mu\nu}(X)$: for ac the transfer is $t_a = (p_a - p_c)^2$, for bd it is $t_b = (p_b - p_d)^2$. If both

are explicitly marked, then the amplitude

$$\mathcal{M}_{\{I\}}^{bd,ac} = ie^2 (G_{e,\mu}^W)_{[ba]} (G_{\nu}^{W,\mu})_{[cd]} \quad (3.12)$$

has to be used.

We split the above expression into soft IR parts proportional to $(\not{p} \pm m)$ and non-IR parts proportional to \not{k}_1 . Employing the completeness relations of eq. (A14) from ref. [4] to those parts we obtain:

$$\begin{aligned} \mathcal{M}_{\{I\}}^{(p k_1)}_{(\lambda \sigma_1)} = & -\frac{eQ_e}{2k_1 p_a} \sum_{\rho} \mathfrak{B}^{[p_b p_a]}_{[\lambda_b \rho_a]} [cd] U^{[p_a k_1 p_a]}_{[\rho_a \sigma_1 \lambda_a]} + \frac{eQ_e}{2k_1 p_b} \sum_{\rho} V^{[p_b k_1 p_b]}_{[\lambda_b \sigma_1 \rho_b]} \mathfrak{B}^{[p_b p_a]}_{[\rho_b \lambda_a]} [cd] \\ & + \frac{eQ_e}{2k_1 p_a} \sum_{\rho} \mathfrak{B}^{[p_b k_1]}_{[\lambda_b \rho]} [cd] U^{[k_1 k_1 p_a]}_{[\rho \sigma_1 \lambda_a]} - \frac{eQ_e}{2k_1 p_b} \sum_{\rho} V^{[p_b k_1 k_1]}_{[\lambda_b \sigma_1 \rho]} \mathfrak{B}^{[k_1 p_a]}_{[\rho \lambda_a]} [cd] \\ & + \mathcal{M}_{WW\gamma}^1 + \mathcal{M}_{WW\gamma}^2 + \mathcal{M}_{WW\gamma}^3. \end{aligned} \quad (3.13)$$

The term $\mathcal{M}_{WW\gamma}$ corresponds to the last three lines⁸ of eq. (3.8). These contributions are also IR-finite. At this stage we keep transfers in the t -channel propagators, which depend on the way how the photon is attached to the fermion line. The summations in the first two terms get eliminated by the diagonality property of U and V (see also ref. [4]) and we obtain

$$\begin{aligned} \mathcal{M}^{1\{I\}}_{(\lambda \sigma_1)}^{(p k_1)} = & \mathfrak{s}_{\sigma_1}^{\{I\}}(k_1) \hat{\mathfrak{B}}^{[p]}_{[\lambda]} + r_{\{I\}}^{(p k_1)}_{(\lambda \sigma_1)}, \\ r_{\{I\}}^{(p k_1)}_{(\lambda \sigma_1)} = & r_{\{I\}}^A + (r_{\{I\}}^B + \mathcal{M}_{WW\gamma}^1) + (\mathcal{M}_{WW\gamma}^2 + \mathcal{M}_{WW\gamma}^3) \\ r_{\{I\}}^A_{(\lambda \sigma_1)}^{(p k_1)} = & + \frac{eQ_e}{2k_1 p_a} \sum_{\rho} \mathfrak{B}^{[p_b k_1]}_{[\lambda_b \rho]} [cd] U^{[k_1 k_1 p_a]}_{[\rho \sigma_1 \lambda_a]} - \frac{eQ_e}{2k_1 p_b} \sum_{\rho} V^{[p_b k_1 k_1]}_{[\lambda_b \sigma_1 \rho]} \mathfrak{B}^{[k_1 p_a]}_{[\rho \lambda_a]} [cd], \\ r_{\{I\}}^B_{(\lambda \sigma_1)}^{(p k_1)} = & - \frac{eQ_e}{2k_1 p_a} \sum_{\rho} \bar{\mathfrak{B}}^{[p_b p_a]}_{[\lambda_b \rho_a]} [cd] U^{[p_a k_1 p_a]}_{[\rho_a \sigma_1 \lambda_a]} + \frac{eQ_e}{2k_1 p_b} \sum_{\rho} V^{[p_b k_1 p_b]}_{[\lambda_b \sigma_1 \rho_b]} \bar{\mathfrak{B}}^{[p_b p_a]}_{[\rho_b \lambda_a]} [cd] \\ \mathfrak{s}_{\sigma_1}^{\{I\}}(k_1) = & - eQ_e \frac{b_{\sigma_1}(k_1, p_a)}{2k_1 p_a} + eQ_e \frac{b_{\sigma_1}(k_1, p_b)}{2k_1 p_b} \quad . \end{aligned} \quad (3.14)$$

The soft part is now clearly separated from the remaining non-IR part, necessary for the CEEX. In $\hat{\mathfrak{B}}^{[p]}_{[\lambda]}$ we use an auxiliary fixed transfer t_0 , independent of the place where the photon is attached to the fermion line. In $\bar{\mathfrak{B}}$ we provide the residual contribution calculated as a difference of the expression calculated with the true t -transfers t_a , t_b and the auxiliary one t_0 , common to all parts of the amplitude. Note that $\mathfrak{B} = \hat{\mathfrak{B}} + \bar{\mathfrak{B}}$.

⁸The term $\mathcal{M}_{WW\gamma}^1 + \mathcal{M}_{WW\gamma}^2 + \mathcal{M}_{WW\gamma}^3$ originates from the $WW\gamma$ vertex

$$-ie[g_{\mu\nu}(p-q)_{\rho} + g_{\nu\rho}(q-r)_{\mu} + g_{\nu\rho}(r-p)_{\nu}]$$

where all momenta are outgoing, and indices on outgoing lines are paired with momenta as p^{μ} , q^{ν} , r^{ρ} ; $\mathcal{M}_{WW\gamma}^1$ originates from the term where $g^{\mu\nu}$ connects the $e^- - \nu_e$, $e^+ - \bar{\nu}_e$ fermion lines.

3.4 One- and two-loop and one-loop–one-real-photon QED corrections

In both the one- and two-loop virtual corrections we use the same formulae as for the s -channel. This is a very convenient approximation, because it simply requires the W -exchange amplitudes to be multiplied by already known functions. As a consequence, the YFS form factor as well as the W contributions to the $\beta_0^{(1,2)}$ functions are readily available within the \mathcal{KKMC} environment.

The one-loop, complete, virtual electroweak W -exchange contributions to the $\beta_0^{(1,2)}$ functions are known. They are given by the difference between the exact contribution and the one for the s -channel, which is given in eq. (2.18). The above virtual W -exchange one-loop contribution to $\beta_0^{(1,2)}$ does not include any numerically sizeable terms with respect to the scale of the term defined in eq. (2.18). In the program, the one-loop W -exchange contribution to $\beta_0^{(1,2)}$ is located in what we call the electroweak W form factor.

Encouraged by the smallness of the above W -exchange one-loop virtual contribution to $\beta_0^{(1,2)}$, and inspired by the contact interaction approximation, we assume that the same is true for two-loop- and one-loop–one-real-photon QED corrections in the complete $\beta_0^{(1,2)}$. At this stage we do not have the complete calculation for $\beta_0^{(1,2)}$. We assume that the approximate $\beta_0^{(1,2)}$ discussed above and used in this work differ from the complete ones by numerically small $\mathcal{O}(\alpha^2)$ terms; see also [21]. We will thus use the same s -channel one-loop contribution to $\beta_0^{(1,2)}$ for the W -exchange amplitudes. This also makes sense because important leading-logarithmic photonic corrections are universal, i.e. the same for any hard process.

The above approximation is, of course, our main source of theoretical uncertainty, which we estimate to be of the order of 1% of the cross-sections of the single-photon observables. As a guide in estimating the size of the above uncertainty for a given $\bar{\nu}\nu(n\gamma)$ final state, we use conservatively the entire size of the one-loop term defined in eq. (2.18).

3.5 Double-photon matrix elements

Complete double-bremsstrahlung spin amplitudes are at present included. Their contribution, as we can see later, turns out to be rather small. We will discuss these exact two-photon amplitudes elsewhere, as well as the related questions of the numerical stability; see the similar discussion for the single-bremsstrahlung amplitude described in the next section. At present, the extensive tests of the type we performed for the s -channel amplitudes, e.g. with the calculation based on ref. [22], are not yet completed. Gauge invariance was used as a main test, so far. We have noticed numerical stability problems, we could not use the complete amplitudes in cases when the photon transverse momenta were smaller than some fraction of the electron mass; however, we have checked (for a statistics of 800,000 events) that this effect is of no numerical relevance.

3.6 Implementation of photon emission for W -exchange in \mathcal{KKMC}

Let us now inspect formula (3.14) (see also fig. 1). It can be divided into three separately gauge-invariant parts. The first gauge invariant part is formed out of the contributions from

diagrams (1) and (2) and diagrams (3) and (4) with the common effective transfer⁹ t_0 : $\mathfrak{s}_{\sigma_1}^{\{I\}}(k_1)\mathfrak{B}^{[p]}_{[\lambda]} + r_{\{I\}}^A$. The second gauge-invariant part includes the contributions from diagrams (3) and (4), responsible for the restoration of true t_a and t_b transfers in place of t_0 , combined with part of diagram (5). It also includes the expression $r_{\{I\}}^B + \mathcal{M}_{WW\gamma}^1$ of eq. (3.14). The third gauge-invariant part is formed out of the remaining two expressions $\mathcal{M}_{WW\gamma}^2 + \mathcal{M}_{WW\gamma}^3$ in eq. (3.14).

The formula of eq. (3.14) requires an additional refinement in cases when more than one photon are present in the event. In such a case the contribution $r_{\{I\}}^B + \mathcal{M}_{WW\gamma}^1$ would lose gauge invariance because of a “non conservation” of the four momenta¹⁰ $p_a + p_b \neq p_c + p_d + k_1$. This is cured as follows: if the momentum carried by other photons is in the same hemisphere as p_a , we choose $t_a = (p_b - k_1 - p_d)^2$, $t_b = (p_b - p_d)^2$ and $\epsilon_t = 2\epsilon_{\sigma_1}^{\mu,*}(k_1) \cdot (p_b - p_d)_\mu$; otherwise we assign $t_a = (p_a - p_c)^2$, $t_b = (p_a - k_1 - p_c)^2$ and $\epsilon_t = 2\epsilon_{\sigma_1}^{\mu,*}(k_1) \cdot (p_c - p_a)_\mu$. In addition, the expression $\mathcal{M}_{WW\gamma}^1$ is modified as follows:

$$\mathcal{M}^1 \left(\frac{p k_1}{\lambda \sigma_1} \right) = +e \hat{\mathfrak{B}} \left[\frac{p_b p_a}{\lambda_b \rho_a} \right] \epsilon_t \frac{t_0 - M_W^2}{(t_a - M_W^2)(t_b - M_W^2)}, \quad (3.15)$$

which coincides with the original expression, if additional photons are absent. Also, if the additional photons are collinear with beams, then this choice is consistent with including them into an “effective beam”, in agreement with the principles of the leading-logarithmic approximation.

3.7 Additional pair correction

The effects from the emission of real charged pairs accompanying the $\nu\bar{\nu}\gamma$ final states may be especially important, because they may change cross sections and distributions through the non-trivial experimental event selection (cuts). It should be kept in mind that the typical experimental event selection for the neutrino final state requires that there be no charged track in the detector (veto). Virtual corrections due to fermion loops in the vertex functions are included in the \mathcal{KK} MC, and can be switched on as explained in the program documentation. The corresponding real pair emission then needs to be added also. This can be done by means of a separate Monte Carlo generation using any massive four-fermion MC event generator, for example KORALW [23].

3.8 Numerical tests using semi-analytical calculations

Once all necessary ingredients of the \mathcal{KK} Monte Carlo program are explained, let us start numerical studies, first for the inclusive quantities, that is for the integrated cross sections.

⁹ In the program, this part of the amplitude is calculated in subroutine `GPS_HiniPlus` and in `GPS_HiniPlusW`; variables `Csum1`, `Csum2`. The contributions $(r_{\{I\}}^B + \mathcal{M}_{WW\gamma}^1)$ and $(\mathcal{M}_{WW\gamma}^2 + \mathcal{M}_{WW\gamma}^3)$, defined later in the text, are calculated as variables `Csum3` and `Csum4` of subroutine `GPS_HiniPlusW`.

¹⁰ For pure s -channel amplitudes this complication is absent; the propagators of the internal vector bosons do not depend on the individual photon momenta, rather on the momenta of the external fermions only, see ref. [4] for details.

In table 2 we show comparisons of results from three programs: \mathcal{KK} MC, \mathcal{KK} sem and ZFITTER. We see good agreement in all three final states, $\nu_{\mu,\tau}$ and μ . Only in the case of ν_e ($v_{max} = 0.90; 0.99$) was the agreement less satisfactory. These comparisons provide an important technical test of our program, although these observables are, of course, academic; their definition requires cuts and tagging of invisible neutrinos.

Table 2: The comparison of three programs: \mathcal{KK} MC, \mathcal{KK} sem, and ZFITTER.

<i>f</i>	(a) \mathcal{KK} sem	(b) CEEX2/t1	(c) ZFITTER 6.36	(b-a)/a	(c-a)/a
$\sigma(v_{max})[\text{pb}], v_{max} = 0.01, 189\text{GeV}$					
ν_e	25.2091 ± 0.0000	25.2351 ± 0.0142	25.2127 ± 0.0000	0.0010 ± 0.0006	0.0001
ν_μ	0.7377 ± 0.0000	0.7383 ± 0.0018	0.7376 ± 0.0000	0.0008 ± 0.0024	-0.0001
ν_τ	0.7377 ± 0.0000	0.7384 ± 0.0018	0.7376 ± 0.0000	0.0009 ± 0.0024	-0.0001
μ	2.1645 ± 0.0000	2.1635 ± 0.0024	2.1682 ± 0.0000	-0.0005 ± 0.0011	0.0017
$\sigma(v_{max})[\text{pb}], v_{max} = 0.10, 189\text{GeV}$					
ν_e	32.5172 ± 0.0000	32.5312 ± 0.0153	32.5572 ± 0.0000	0.0004 ± 0.0005	0.0012
ν_μ	0.9671 ± 0.0000	0.9674 ± 0.0019	0.9669 ± 0.0000	0.0004 ± 0.0020	-0.0002
ν_τ	0.9671 ± 0.0000	0.9678 ± 0.0019	0.9669 ± 0.0000	0.0007 ± 0.0020	-0.0002
μ	2.8227 ± 0.0000	2.8234 ± 0.0027	2.8276 ± 0.0000	0.0003 ± 0.0009	0.0017
$\sigma(v_{max})[\text{pb}], v_{max} = 0.80, 189\text{GeV}$					
ν_e	45.5520 ± 0.0000	45.4818 ± 0.0166	45.6423 ± 0.0000	-0.0015 ± 0.0004	0.0020
ν_μ	7.6919 ± 0.0000	7.7001 ± 0.0039	7.6907 ± 0.0000	0.0011 ± 0.0005	-0.0002
ν_τ	7.6919 ± 0.0000	7.7018 ± 0.0039	7.6907 ± 0.0000	0.0013 ± 0.0005	-0.0002
μ	6.9623 ± 0.0000	6.9658 ± 0.0031	6.9740 ± 0.0000	0.0005 ± 0.0005	0.0017
$\sigma(v_{max})[\text{pb}], v_{max} = 0.90, 189\text{GeV}$					
ν_e	45.6631 ± 0.0000	45.6038 ± 0.0166	46.1404 ± 0.0000	-0.0013 ± 0.0004	0.0105
ν_μ	7.9012 ± 0.0000	7.9100 ± 0.0039	7.9008 ± 0.0000	0.0011 ± 0.0005	-0.0001
ν_τ	7.9012 ± 0.0000	7.9117 ± 0.0039	7.9008 ± 0.0000	0.0013 ± 0.0005	-0.0001
μ	7.2070 ± 0.0000	7.2115 ± 0.0032	7.2192 ± 0.0000	0.0006 ± 0.0004	0.0017
$\sigma(v_{max})[\text{pb}], v_{max} = 0.99, 189\text{GeV}$					
ν_e	45.6770 ± 0.0000	45.6247 ± 0.0166	46.3844 ± 0.0000	-0.0011 ± 0.0004	0.0155
ν_μ	7.9102 ± 0.0000	7.9190 ± 0.0039	7.9100 ± 0.0000	0.0011 ± 0.0005	-0.0000
ν_τ	7.9102 ± 0.0000	7.9207 ± 0.0039	7.9100 ± 0.0000	0.0013 ± 0.0005	-0.0000
μ	7.6156 ± 0.0000	7.6234 ± 0.0032	7.6282 ± 0.0000	0.0010 ± 0.0004	0.0017

4 Numerical results from \mathcal{KK} MC and KORALZ

Let us now present new important numerical results using observables (event selections) defined in the LEP2 MC Workshop [1], without any modifications. These observables were defined to suit the needs of all LEP experiments and to match their particular experimental studies.

Observables can be divided into two groups: single photon tagged observables **Nu1**, **Nu11**, **Nu12**, **Nu13**, **Nu3**, **Nu4g**, **Nu7**, where the precision target required by experiments is 0.5%, and the observables with two observed photons **Nu2**, **Nu14**, **Nu5**, **Nu6**, **Nu8**, **Nu9**, **Nu10**, where the precision target is 2%, see ref. [1].

Numerical results are collected in Table 3. For every observable and a total energy of 189 GeV, numerical results are collected from the \mathcal{KK} MC with the exact double hard photon

matrix element (CEEX2) and the exact single matrix element only (CEEX1). First, we can conclude that the predictions from KORALZ presented during the LEP2 MC Workshop and for all neutrino observables were generally correct within 4%, in agreement with what has been declared. One can even get an impression that the agreement is better, of the order of 2%. This, however, is misleading, since these small differences were due to accidental cancellations of several effects, all of them of the order of 2–3% .

Let us now discuss results from the \mathcal{KK} MC with the various options for the matrix element, having in mind an estimate of the theoretical uncertainties. We have found for all observables that the correction from additional virtual fermion pairs was systematically -0.6% . (The corresponding entries are not included in the actual version of table 3.) Since the virtual fermion pairs contribution is rather small, in comparison with other uncertainties, we will use the size of the above virtual correction of 0.6% as a conservative estimate of the corresponding systematic error. Concerning the missing higher order QED contributions (see section 3.4) we estimate it to be 1% for ν_e and 0.5% for other neutrinos. Finally we take 0.4% as for the systematic uncertainty of electroweak corrections of ZFITTER. The final uncertainty for the single-photon observables is thus estimated to be 1.3% for electron neutrino final states and about 0.8% for the other neutrino species.

The uncertainty for observables with two tagged hard photons is higher, probably of the order of¹¹ 5%. As a numerical input we use standard initialization parameters of the \mathcal{KK} MC defined in ref. [2].

5 Conclusions

We have extended the Monte Carlo program \mathcal{KK} to the neutrino mode. The systematic error is estimated to be 1.3% for $\nu_e \bar{\nu}_e \gamma$ and 0.8% for $\nu_\mu \bar{\nu}_\mu \gamma$ and $\nu_\tau \bar{\nu}_\tau \gamma$. For observables with two observed photons we estimate the uncertainty to be about 5%. These new improved results were obtained thanks to the inclusion of non-photonic electroweak corrections of the ZFITTER package [5, 6] and due to newly constructed, exact, single and double emission photon amplitudes in the \mathcal{KK} MC for the contribution with the t -channel W exchange. The virtual corrections for the W exchange are at present introduced in the approximated form. The exponentiation scheme CEEX is the same as in the original \mathcal{KK} MC program of refs. [2–4].

Let us also note that in the other Monte Carlo programs available in the literature for the neutrino channel, see eg. refs. [24, 25], the exact double-photon bremsstrahlung amplitudes are also included. Direct comparisons with these programs should be done at a certain point. This could provide an independent cross check of our double-photon matrix element and may also shed light on certain non-negligible differences between the results for the neutrino channel LEP observables collected from various MC event generators during the LEP2 MC Workshop [1]. Therefore, a better answer could be provided on the total theoretical and technical uncertainties in these calculations.

¹¹Such an estimate was obtained by switching on and off the double-photon contribution to the matrix element. See entries CEEX2 and CEEX1 in Table 3. Also, the different options of reduction procedures could be compared and the corresponding contribution to the net uncertainties could be reduced. We leave, however, these points for future studies.

Acknowledgements

Z.W. would like to thank Paul Colas for his encouraging to start studying the phenomenology of $e^+e^- \rightarrow \bar{\nu}\nu\gamma$ in the early 90's. Useful discussions with B. Bloch, J. Boucrot, A. Jacholkowska, W. Płaczek, M. Skrzypek and B.F.L. Ward are also acknowledged.

References

- [1] Two Fermion Working Group Collaboration, M. Kobel *et al.*, in CERN 2000-009, “Reports of the working groups on precision calculation for LEP-2 physics”, Proceedings, Monte Carlo Workshop, Geneva, Switzerland, 1999-2000, eds. S. Jadach, G. Passarino and R. Pittau, [hep-ph/0007180](#).
- [2] S. Jadach, B. F. L. Ward, and Z. Was, *Comput. Phys. Commun.* **130** (2000) 260, [hep-ph/9912214](#).
- [3] S. Jadach, B. F. L. Ward, and Z. Was, *Phys. Lett.* **B449** (1999) 97–108, [hep-ph/9905453](#).
- [4] S. Jadach, B. F. L. Ward, and Z. Was, *Phys. Rev.* **D63** (2001) 113009, [hep-ph/0006359](#).
- [5] D. Bardin, P. Christova, M. Jack, L. Kalinovskaya, A. Olshevski, S. Riemann and T. Riemann, *Comput. Phys. Commun.* **133** (2001) 229–395, [hep-ph/9908433](#).
- [6] ZFITTER project, <http://www.ifh.de/~riemann/Zfitter/zf.html>.
- [7] S. Jadach, B. F. L. Ward, and Z. Was, *Comput. Phys. Commun.* **124** (2000) 233, [hep-ph/9905205](#).
- [8] S. Jadach, B. F. L. Ward, and Z. Was, *Comput. Phys. Commun.* **79** (1994) 503–522.
- [9] D. Bardin, M. Bilenky, A. Chizhov, O. Fedorenko, S. Ganguli, A. Gurtu, M. Lokajicek, G. Mitselmakher, Olshevsky, J. Ridky, S. Riemann, T. Riemann, M. Sachwitz, A. Sazonov, D. Schaile, Y. Sedykh, and I. S. L. Vertogradov, “ZFITTER v.4.5: An analytical program for fermion pair production in e^+e^- annihilation”, preprint CERN-TH. 6443/92 (1992), [hep-ph/9412201](#).
- [10] A. Arbuzov, D. Bardin, J. Blümlein, L. Kalinovskaya, and T. Riemann, *Comput. Phys. Commun.* **94** (1996) 128, [hep-ph/9511434](#).
- [11] D. Bardin, M. S. Bilenky, G. Mitselmakher, T. Riemann, and M. Sachwitz, *Z. Phys. C44* (1989) 493.
- [12] D. Bardin, G. Passarino, and W. Hollik (eds.), “Reports of the working group on precision calculations for the Z resonance”, report CERN 95–03 (1995).
- [13] D. Bardin, P. Christova, and O. Fedorenko, *Nucl. Phys.* **B197** (1982) 1.

- [14] D. Bardin, C. Burdik, P. Christova, and T. Riemann, “Study of electroweak radiative corrections to deep inelastic scattering at HERA”, submitted to Workshop on Physics at HERA, Hamburg, Germany, Oct 12-14, 1987, JINR Dubna preprint E2-87-595 (1987).
- [15] D. Y. Bardin, K. C. Burdik, P. K. Khristova, and T. Riemann, *Z. Phys. C* **44** (1989) 149.
- [16] D. R. Yennie, S. Frautschi, and H. Suura, *Ann. Phys. (NY)* **13** (1961) 379.
- [17] M. Greco, G. Panchari-Srivastava, and Y. Srivastava, *Phys. Lett.* **56B** (1975) 367.
- [18] M. Greco, G. Panchari-Srivastava, and Y. Srivastava, *Nucl. Phys.* **B171** (1980) 118–140; Erratum: *Nucl. Phys.* **B197** (1982) 543–546.
- [19] R. Kleiss and W. J. Stirling, *Nucl. Phys.* **B262** (1985) 235.
- [20] R. Kleiss and W. J. Stirling, *Phys. Lett.* **B179** (1986) 159.
- [21] F. A. Berends, G. J. H. Burgers, C. Mana, M. Martinez, and W. L. van Neerven, *Nucl. Phys.* **B301** (1988) 583.
- [22] E. Richter-Was, *Z. Phys. C* **61** (1994) 323–340.
- [23] S. Jadach, W. Placzek, M. Skrzypek, B. F. L. Ward, and Z. Was, [hep-ph/0104049](#).
- [24] Y. Kurihara, J. Fujimoto, T. Ishikawa, Y. Shimizu, and T. Munehisa, *Comput. Phys. Commun.* **136** (2001) 250–268, [hep-ph/9908422](#).
- [25] G. Montagna, M. Moretti, O. Nicrosini, M. Osmo, and F. Piccinini, *Phys. Lett.* **B515** (2001) 197–205, [hep-ph/0105120](#).

Table 3: Numerical predictions for observables of the LEP2 MC Workshop at a total energy of 189 GeV (input data of the Workshop). For each observable results are shown in 3 lines: (i) CEEX2 $\mathcal{O}(\alpha^2) \mathcal{K}\mathcal{K}$ MC, (ii) CEEX1 $\mathcal{O}(\alpha^1) \mathcal{K}\mathcal{K}$ MC, (iii) KORALZ MC. The difference δ is shown in the last column: it is the deviation from 1 ($\times 100$) of the ratio of a given result to that of CEEX2.

Label of obs.	Program	Cross section [pb]	δ ratio
Nu1	KKMC CEEX2	$3.1710 \cdot 10^0 \pm 7.43 \cdot 10^{-3}$	
	KKMC CEEX1	$3.2139 \cdot 10^0 \pm 3.85 \cdot 10^{-3}$	1.35
	KORALZ 4.04	$3.2244 \cdot 10^0 \pm 4.34 \cdot 10^{-3}$	1.68
Nu2	KKMC CEEX2	$2.1886 \cdot 10^{-1} \pm 9.26 \cdot 10^{-4}$	
	KKMC CEEX1	$2.1655 \cdot 10^{-1} \pm 8.79 \cdot 10^{-4}$	-1.06
	KORALZ 4.04	$2.1733 \cdot 10^{-1} \pm 1.20 \cdot 10^{-3}$	-0.70
Nu11	KKMC CEEX2	$9.1551 \cdot 10^{-1} \pm 2.26 \cdot 10^{-3}$	
	KKMC CEEX1	$9.1066 \cdot 10^{-1} \pm 2.23 \cdot 10^{-3}$	-0.53
	KORALZ 4.04	$9.1767 \cdot 10^{-1} \pm 2.42 \cdot 10^{-3}$	0.24
Nu12	KKMC CEEX2	$1.8242 \cdot 10^0 \pm 3.09 \cdot 10^{-3}$	
	KKMC CEEX1	$1.8359 \cdot 10^0 \pm 3.07 \cdot 10^{-3}$	0.64
	KORALZ 4.04	$1.8442 \cdot 10^0 \pm 3.37 \cdot 10^{-3}$	1.09
Nu13	KKMC CEEX2	$1.7775 \cdot 10^0 \pm 6.95 \cdot 10^{-3}$	
	KKMC CEEX1	$1.8085 \cdot 10^0 \pm 2.82 \cdot 10^{-3}$	1.75
	KORALZ 4.04	$1.8045 \cdot 10^0 \pm 3.35 \cdot 10^{-3}$	1.52
Nu14	KKMC CEEX2	$2.0634 \cdot 10^{-1} \pm 9.02 \cdot 10^{-4}$	
	KKMC CEEX1	$2.0267 \cdot 10^{-1} \pm 8.40 \cdot 10^{-4}$	-1.78
	KORALZ 4.04	$2.0121 \cdot 10^{-1} \pm 1.15 \cdot 10^{-3}$	-2.49
Nu3	KKMC CEEX2	$4.2434 \cdot 10^0 \pm 7.78 \cdot 10^{-3}$	
	KKMC CEEX1	$4.2912 \cdot 10^0 \pm 4.48 \cdot 10^{-3}$	1.13
	KORALZ 4.04	$4.2885 \cdot 10^0 \pm 4.89 \cdot 10^{-3}$	1.06
Nu5	KKMC CEEX2	$1.2128 \cdot 10^{-1} \pm 6.77 \cdot 10^{-4}$	
	KKMC CEEX1	$1.1912 \cdot 10^{-1} \pm 6.26 \cdot 10^{-4}$	-1.78
	KORALZ 4.04	$1.1850 \cdot 10^{-1} \pm 8.83 \cdot 10^{-4}$	-2.30
Nu6	KKMC CEEX2	$5.7331 \cdot 10^{-2} \pm 4.64 \cdot 10^{-4}$	
	KKMC CEEX1	$5.5817 \cdot 10^{-2} \pm 4.22 \cdot 10^{-4}$	-2.64
	KORALZ 4.04	$5.6543 \cdot 10^{-2} \pm 6.11 \cdot 10^{-4}$	-1.37
Nu7	KKMC CEEX2	$4.4676 \cdot 10^0 \pm 7.82 \cdot 10^{-3}$	
	KKMC CEEX1	$4.5206 \cdot 10^0 \pm 4.54 \cdot 10^{-3}$	1.19
	KORALZ 4.04	$4.5109 \cdot 10^0 \pm 5.00 \cdot 10^{-3}$	0.97
Nu8	KKMC CEEX2	$1.7593 \cdot 10^{-1} \pm 8.31 \cdot 10^{-4}$	
	KKMC CEEX1	$1.7162 \cdot 10^{-1} \pm 7.63 \cdot 10^{-4}$	-2.45
	KORALZ 4.04	$1.7074 \cdot 10^{-1} \pm 1.06 \cdot 10^{-3}$	-2.95
Nu9	KKMC CEEX2	$7.6434 \cdot 10^{-2} \pm 5.39 \cdot 10^{-4}$	
	KKMC CEEX1	$7.4473 \cdot 10^{-2} \pm 4.89 \cdot 10^{-4}$	-2.56
	KORALZ 4.04	$7.4208 \cdot 10^{-2} \pm 7.00 \cdot 10^{-4}$	-2.91
Nu10	KKMC CEEX2	$2.5362 \cdot 10^{-1} \pm 1.00 \cdot 10^{-3}$	
	KKMC CEEX1	$2.5107 \cdot 10^{-1} \pm 9.39 \cdot 10^{-4}$	-1.01
	KORALZ 4.04	$2.5040 \cdot 10^{-1} \pm 1.28 \cdot 10^{-3}$	-1.27
Nu4g	KKMC CEEX2	$1.9091 \cdot 10^0 \pm 6.99 \cdot 10^{-3}$	
	KKMC CEEX1	$1.9379 \cdot 10^0 \pm 2.92 \cdot 10^{-3}$	1.51
	KORALZ 4.04	$1.9398 \cdot 10^0 \pm 3.46 \cdot 10^{-3}$	1.61